PAPER • **OPEN ACCESS**

Experimental optimisation of O-ring resonator Q-factor for on-chip spontaneous four wave mixing

To cite this article: P An *et al* 2018 *J. Phys.: Conf. Ser.* **1124** 051047

Experimental optimisation of O-ring resonator Q-factor for on-chip spontaneous four wave mixing

P An[1, 2], V Kovalyuk[1,2], A Golikov[1], E Zubkova[1,2], S Ferrari[3,4], A Korneev[1,5], W Pernice[3,4], G Goltsman[1,2,6]
[1]Department of Physics, Moscow State Pedagogical University, 119992, Russia
[2]Zavoisky Physical-Technical Institute of the Russian Academy of Sciences, 420029, Russia
[3]Institute of Physics, University of Münster, 48149, Germany
[4]CeNTech - Center for Nanotechnology, University of Münster, 48149, Germany
[5]Moscow Institute of Physics and Technology (State University), 141700, Russia
[6]National Research University Higher School of Economics, Moscow 101000, Russia

Abstract. In this paper we experimentally studied the influence of geometrical parameters of the planar O-ring resonators on its Q-factor and losses. We systematically changed the gap between the bus waveguide and the ring, as well as the width of the ring. We found the highest Q = 5×10^5 for gap 2.0 µm and the ring width 2 µm. This work is important for further on-chip SFWM applications since the generation rate of the biphoton field strongly depends on the quality factor as Q^3

1. Introduction
Planar optical ring resonators (ORRs) are very powerful devices for different applications, including optical filtering [1], biology [2], photon pair generation [3] and generation of high-dimensional entangled quantum states [4] . One of the most important parameters of the ORR are waveguide losses and quality factor (Q-factor). In this work we experimentally study dependence of ORR Q-factor and internal losses on two main geometrical parameters: gap (G) between single mode bus waveguide and O-ring waveguide width (W_r).

2. Device designing and fabrication
We fabricated a 2D array of devices with two sweep parameters: $G = 0.1\div2.0$ µm and $W_r = 1.2\div2.0$ µm and designed them using a self-made Python programming script for positive e-beam lithography processing. The ttypical element of the array consisted of two focusing grating couplers (FGCs) for input and output light awaveguide bus with fixed width of 1µm width and a O-ring with fixed radius of 50µm, located at a variable distance (gap) from the bus waveguide as depicted inFigure 1(a). The total number of devices inside the array was 200. We used commercial available Si wafers with 450 nm Si_3N_4 surface as an optical layer, and SiO_2 layer with 2600 nm as an optical buffer between Si and Si_3N_4 .

Fabrication process included one step e-beam lithography with current of electron beam of 25 pA and 30 kV accelerate voltage and included a proximity effect correction using NanoMaker software. A positive e-beam resist ZEP 520A was spin coated at a speed of 4000 rpm to achieve a nominal thickness of 400 nm. We developed ZEP 520A in O-Xylene for 50 sec at a temperature of 25°C after the exposure. Dark field optical microcopy was used for controlling of the development procedure. Reactive ion etching process (RIE) was used for waveguide finalizing in argon and CHF_3 gas mixture. We etched only the half of height of the optical layer (rib waveguides) due to better geometry parameters reproducibility. Finally, ZEP 520A was removed by oxygen plasma cleaning.

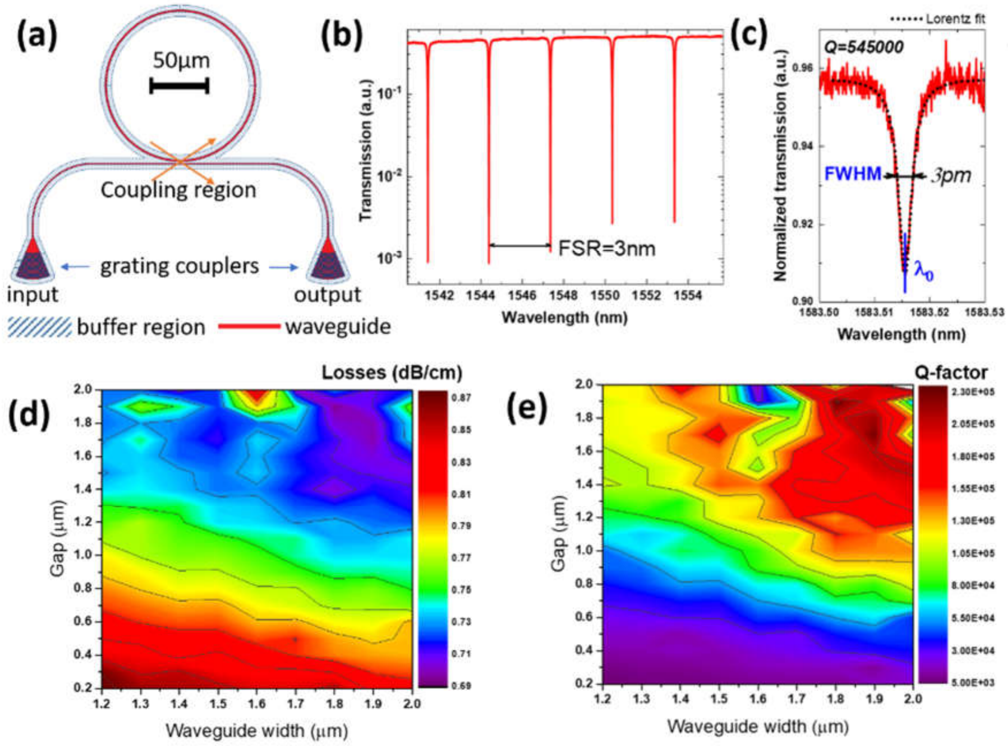

Figure 1(a-e). (a) Design of the planar optical resonator (ORR); **(b)** Transmission spectrum of ORR; **(c)** Single resonance peak demonstrated Q-factor over 5×10^5; **(d)** Color contour map of the optical losses vs gap and ring waveguide width; **(e)** Color contour map of the Q-factor vs gap and ring waveguide width

3. Experimental setup

Our experimental setup consisted with tunable laser source (New Focus TLB-6600) for tune the light in the range of 1510÷1620 nm, polarization controller for adjusting polarization, 3D mechanical stage with piezo motors for precision geometrical aligning of FGCs and light from fibers array [5], as well as a fast photodetector for optical power measurementsAdditionally to the main ORRs, we measured test devices without rings, fabricated in the same technology process. We subtract the spectrum of FGC from ORRs spectra, obtaining the normalized O-ring transmission spectra.

4. Methods and results

Typical optical transmission of one of the ORR is shown in Figure 1(b). We found, that the measured free spectral range (FSR) has a good agreement with the theoretical equation:

$$FSR = \Delta\lambda = \frac{\lambda^2}{n_g L}, \quad (1)$$

where Δλ is the wavelength difference between two resonances, n_g is group refractive index and $\boldsymbol{L = 2\pi R}$ is length of the ring (R = 63.73 µm and $n_g \approx 2$).

The Q-factor of the O-ring resonator is proportional to numbers of oscillations of the field before the stored optical power depletes to $1/e$ on respect to the initial power: $\boldsymbol{P(x) = P_0 e^{-\alpha x}}$.

IOP Conf. Series: Journal of Physics: Conf. Series **1124** (2018) 051047 doi:10.1088/1742-6596/1124/5/051047

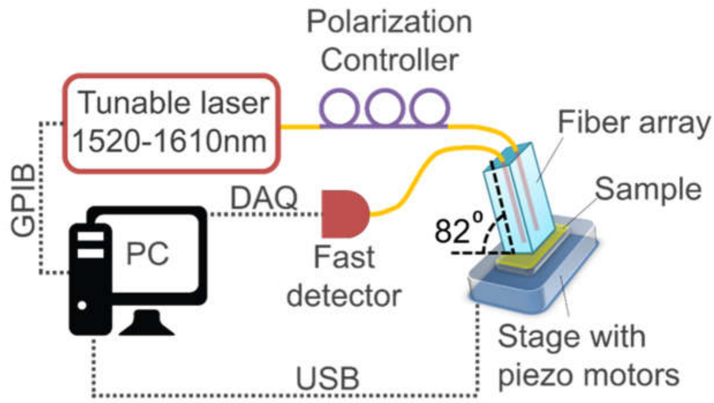

Figure 2. Experimental setup for the measurements of the transmission spectra of ORRs. Light from the tunable laser source is aligned with the ORRs using a fiber array and 3D stage with piezo motors. Light, passing thought structures, was detected by a fast photodetector. The photodetectros signal was recorded using a NI DAQ system. A polarization controller serves to match the the direction of polarization of the incident wave and the FGC.

The number of oscillations, are determinated by the losses α in the ring. The formal expression for the intrinsic Q-factor is:

$$Q_{int} = \frac{2\pi n_g}{\alpha\lambda}. \tag{2}$$

Q_{int} cannot be directly measured from the transmission spectra, but can be extrapolated by determining the loaded quality factor Q_{loaded}.

In order to extrapolate $\mathbf{Q_{int}}$ we first determined the loaded quality factor of the resonance peak directly from transmission spectra:

$$Q_{loaded} = \frac{\lambda_0}{FWHM}, \tag{3}$$

where FWHM is the full width half maximum of a resonant peak and $\boldsymbol{\lambda_0}$ is the resonance wavelength (Figure 1(c)). We chose the λ_0 near 1550 nm for all of the structures and resonance Lorentz fitting for the best extracting λ_0 and peak FWHM.

In a second step, we calculated the intrinsic Q-factor of the ring [6]:

$$Q_{int} = \frac{2Q_{loaded}}{1+\sqrt{T_0}}, \tag{4}$$

where T_0 is the fraction of transmitted optical power measured by the photodetector at the resonant wavelength λ_0.

Finally, combining equation (1), (2) and (4) we calculated optical losses α in the ring:

$$\alpha = \frac{2\pi n_g}{Q_{int}\lambda_0} = \frac{\pi\cdot\lambda_0}{FSR\cdot L}\left[FWHM(1+\sqrt{T_0})\right]. \tag{5}$$

In Figure 1(d,e) are shown a color contour map of Q-factor and losses dependencies on G and W_r. The highest Q-factor corresponds the region with the lowest losses pointing to the close to the critical coupling regime [7]. we found devices with higher quality factor value of $Q = 5.45\cdot10^5$, at the resonance wavelength of 1583.5 nm.

5. Conclusions

In conclusion, we studied dependence of ORR Q-factor vs gap between single mode bus waveguide and O-ring with different waveguide width (W_r). We found that lowest losses (~ 0.6 dB/cm) and highest Q-factor (over $2.3\cdot10^5$) at wavelength 1550 nm has the ring with $G = 1.8$µm and $W_r = 1.9$ µm. This results is important for further on-chip SFWM applications since the generation rate of the biphoton field strongly depends on the quality factor as Q^3.

Acknowledgments
P. An, V. Kovalyuk, E. Zubkova and G. Goltsman acknowledge support by the Russian Science Foundation (project No. 16-12-00045; device design and testing). A. Korneev acknowledges support of the Russian Science Foundation (project No. 17-72-30036; nanophotonic circuits modeling) and W. Pernice acknowledges support by the DFG grants PE 1832/1-1 & PE 1832/1-2 and the Helmholtz society through grant HIRG-0005 (fabrication of nanophotonic circuits).

References
[1] Rabus, D. G. et.al. 2002. *IEEE Journal of Selected Topics in Quantum Electronics* **8** 6 1405–1411
[2] Juan-Colás, J. et.al. 2016. *Nature Communications* **7**
[3] E. Engin et.al. 2013 *Opt. Express* **21** 27826-27834
[4] Kues, M. et.al. 2017. *Nature* **546** 7660 622–626
[5] Taillaert D. et. al. 2016 *Japanese Journal of Applied Physics* **45** 8-A 6071–6077
[6] P. Barclay et.al 2005 *Opt. Express* **13** 801-820
[7] Yariv, A. 2002. *IEEE Photonics Technology Letters* **14** 4 483–485